

## Supplementary Information

### **The PD-L1 cellular nanovesicles carrying rapamycin inhibit alloimmune responses in transplantation**

Min Yang<sup>1#</sup>, Zhanxue Xu<sup>1#</sup>, Hailan Yan<sup>1#</sup>, Hsiang-I Tsai<sup>1</sup>, Dandan Su<sup>1</sup>, Fuxia Yan<sup>1</sup>,  
Qiumei Lu<sup>1</sup>, Jianhua Feng<sup>2</sup>, Weiwei Zeng<sup>1</sup>, Lifang Xi<sup>1</sup>, Hualian Zha<sup>1</sup>, Yunzhi Ling<sup>1</sup>,  
Chao He<sup>1</sup>, Yingyi Wu<sup>1</sup>, Xiaowei Xu<sup>3</sup>, Gang Zheng<sup>4</sup>, Gan Liu<sup>1,5\*</sup>, Hongbo Chen<sup>1\*</sup>, Fang  
Cheng<sup>1\*</sup>

1. School of pharmaceutical sciences (Shenzhen), Sun Yat-sen University, Shenzhen, 518107, China

2. Department of Hematology, Zhujiang Hospital, Southern Medical University, Guangzhou, 510280, China

3. Clinical Neuroscience Center, The Seventh Affiliated Hospital of Sun Yat-sen University, Shenzhen, 518000, China

4. XuZhou Central Hospital Affiliated to Medical School of Southeast University, XuZhou, 221000, China

5. Division of Life and Health Sciences, Graduate School at Shenzhen, Tsinghua University, Shenzhen, 518055, China

**\*Correspondence to:** chengf9@mail.sysu.edu.cn (F. Cheng)  
chenhb7@mail.sysu.edu.cn (H. Chen)  
liugan5@mail.sysu.edu.cn (G. Liu)

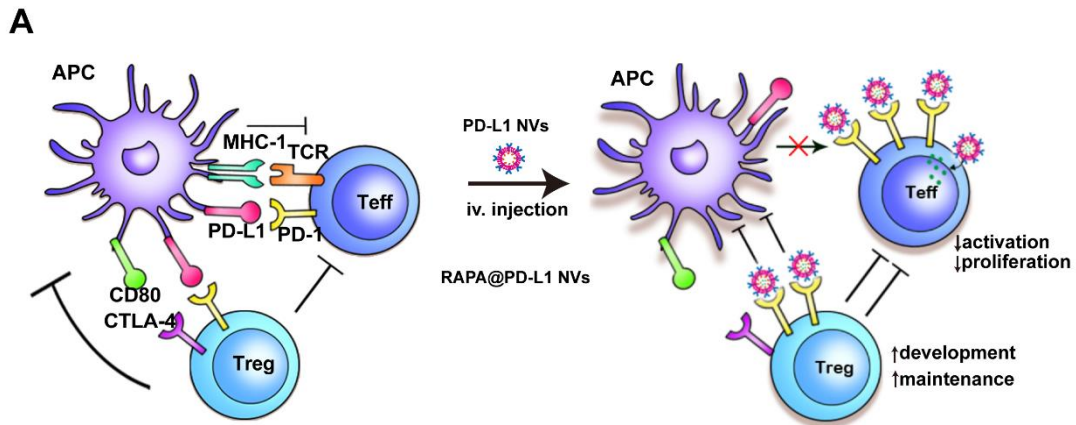


**Figure S1. Schematic diagram of RAPA@PD-L1 NVs.**

(A) Schematic diagram showed the action mechanism of PD-L1 NVs loaded with RAPA (RAPA@PD-L1 NVs).

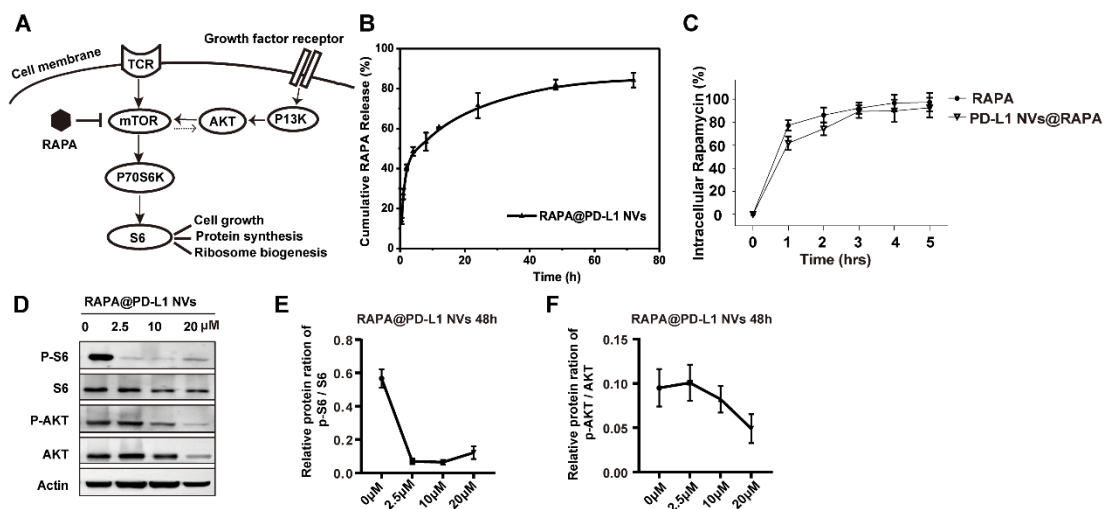


**Figure S2. The action mechanism and uptake of RAPA in cells.**

(A) Mechanisms of RAPA inhibiting AKT/mTOR/p70S6K feedback pathway and impact on T cell proliferation. (B) *In vitro* release of RAPA from the RAPA@PD-L1 NVs. Error bar, mean  $\pm$  SEM (n=3). (C) Uptake of rapamycin in Jurkat cells. Jurkat cells were incubated with 45  $\mu$ g /ml of rapamycin at 37  $^{\circ}$ C during above time. Extracted and purified intracellular rapamycin was detected by HPLC analysis (n=3). (D-F) Representative western blot plots and quantitative analysis of the effect of RAPA at different drug concentrations on the expression of pS6 and pAKT in Jurkat T cells, Error bar, mean  $\pm$  SEM (n=3).

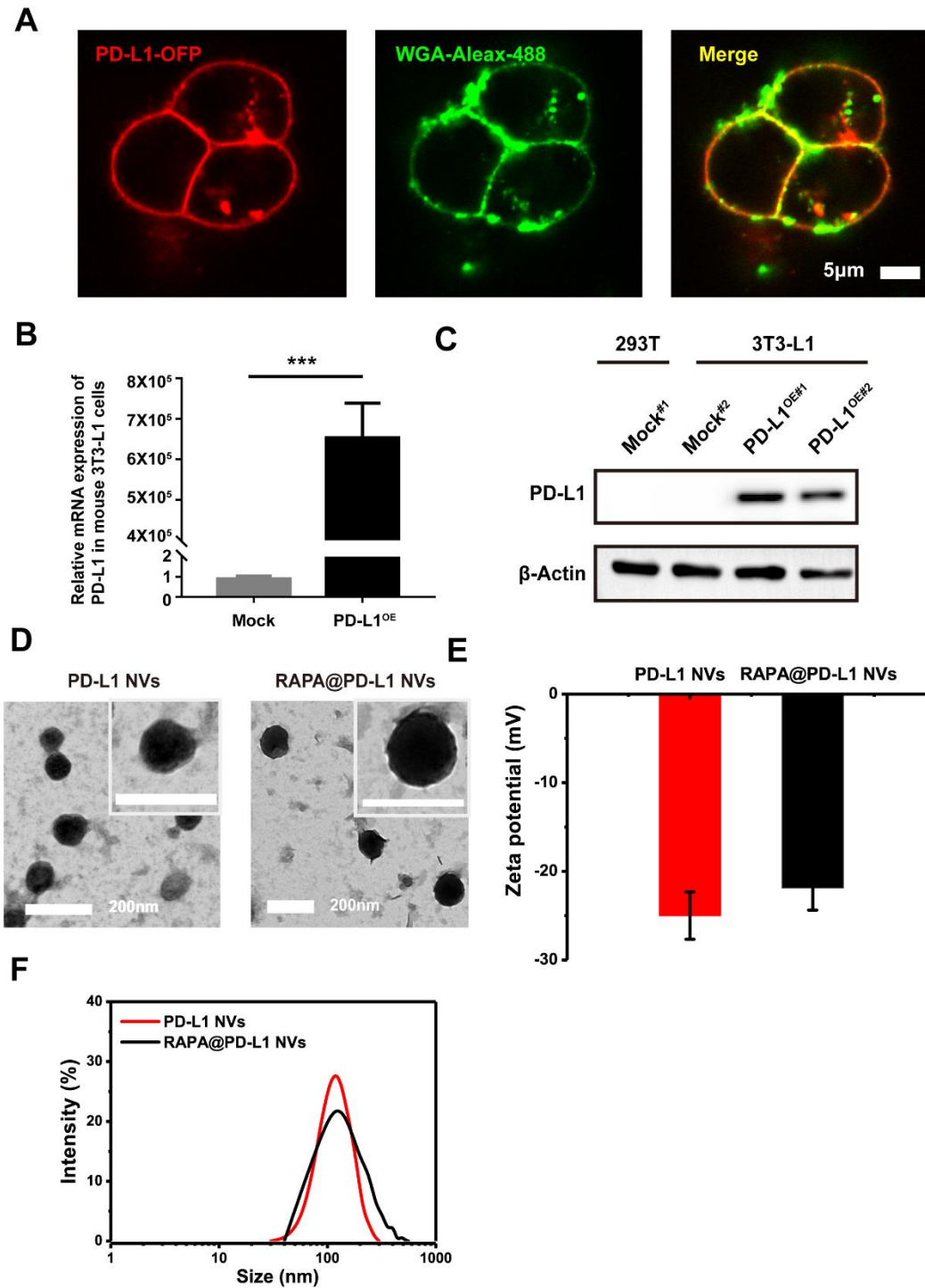


**Figure S3. Construction of mouse 3T3-L1 stable cell line overexpressing PD-L1 proteins on membrane and characterization of PD-L1 NVs.**

(A) Representative confocal images of mouse 3T3-L1 expressing PD-L1-OFP. Scale bar: 5  $\mu$ m. (B) qPCR analysis of PD-L1 mRNA in 3T3L1-PD-L1-OFP cells. (C) Western blotting of mouse PD-L1-OFP expressed on the membrane of the 3T3-L1 cells. (D) The TEM image of mouse PD-L1 NVs and RAPA@PD-L1 NVs. Scale bar: 200

nm. (E-F) The zeta potentials and size distribution of mouse RAPA@PD-L1 NVs/PD-L1 NVs by dynamic light scattering analysis.

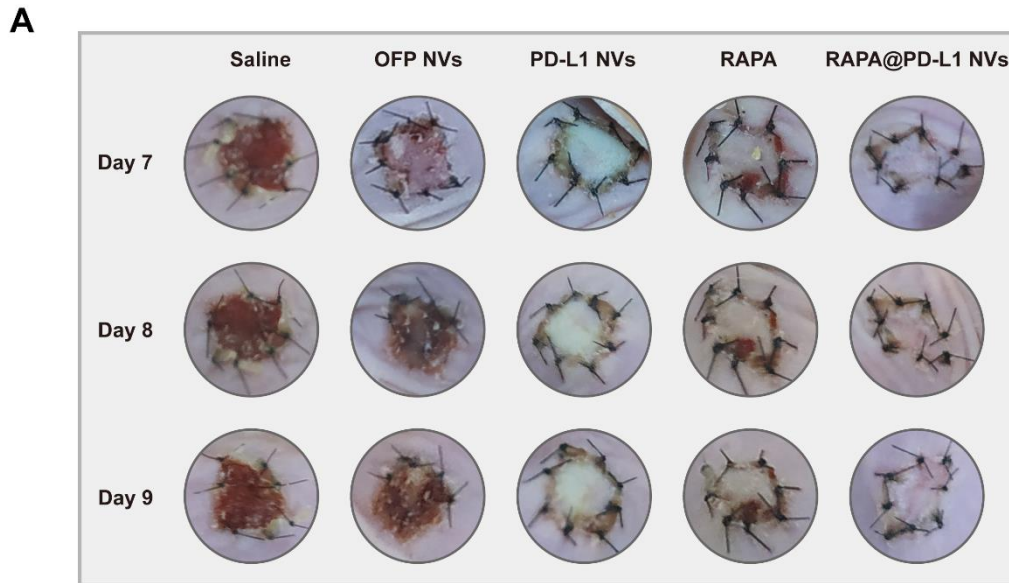


**Figure S4. Time-lapse skin-graft pictures upon treatments.**

(A) The representative skin macro-photographs of mice accepting skin transplantation in Day 7, 8 and 9 upon saline, OFP NVs, PD-L1 NVs, RAPA or RAPA@PD-L1 NVs treatment based on a 5-point skin scoring system. The endpoint of the mouse allograft survival is defined as complete rejection of the allograft (score 5).

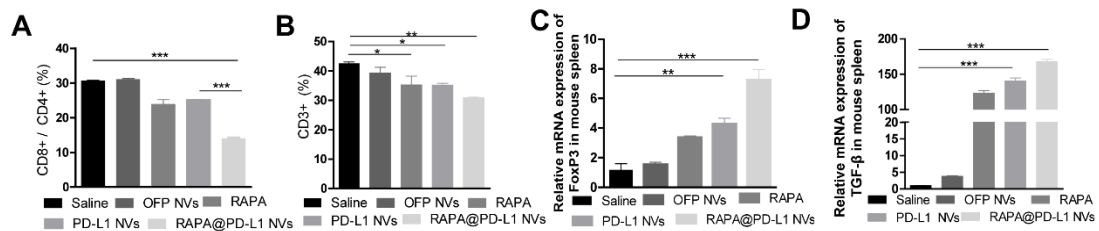


**Figure S5. The quantitative analysis of T cells and related factors levels detected by qPCR.**

(A-B) The quantitative analysis of CD8<sup>+</sup>/CD4<sup>+</sup> T cell ratio and responding T cell ratio from mouse spleen samples of different drug injection groups. (C-D) FoxP3 and TGF-β levels from spleen were measured by qPCR in skin-graft mice. Error bar, mean ±

SEM (n=3). (A-D) One-way ANOVA with Tukey posthoc test analyses were performed. \*P < 0.05, \*\*P < 0.01, \*\*\*P < 0.001

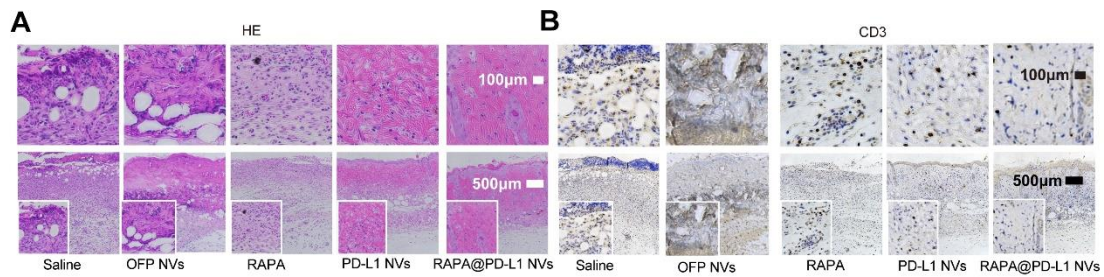


**Figure S6. *In vivo* images of graft-skin for HE staining and Immunofluorescence**  
(A-B) Representative images of HE staining and Immunofluorescence of graft-skin for CD3 antibody. Scale bar: 100 µm.